

Polarization-Based Zero Forcing with Channel Estimation

Thomas G. Pratt^a, Hrishikesh Tapse^a, Robert Baxley^b, Brett Walkenhorst^b, and Guillermo Acosta-Marum^b

Email: {tp Pratt@nd.edu, htapse@nd.edu, rbaxley@gti.gatech.edu, brett.guillermo.acosta-marum@gti.gatech.edu}

^aUniversity of Notre Dame
Notre Dame, IN 46556

^bGeorgia Tech Research Institute
Atlanta, Georgia 30318

Abstract — A robust, low-complexity polarization-based zero forcing (ZF) filtering technique is proposed for the suppression of asynchronous, co-channel interference (ACCI) that cannot be resolved from the desired signal in angle. Suppression is achieved in the polarization-frequency dimension and requires either channel estimates or *relative* channel estimates for the orthogonally-polarized components of the interference signal. We consider the impact of background co-channel interference (BCCI) during channel estimation of the ACCI signal and show that the suppression performance of the ZF filter degrades with the quality of the ACCI channel estimates, i.e., the performance is approximately limited to the power ratio between the ACCI and the BCCI signals. Methods to counteract the impact of the BCCI are considered that exploit the correlation inherent in the polarization-frequency domain. One approach involves smoothing in the frequency domain, which is shown to yield improved channel estimates for ZF filtering and cancellation performance gains. Another strategy is also considered that monitors ACCI signal depolarization induced by the BCCI to identify the ACCI signal channel estimates with the least disturbance from the BCCI. The methods are demonstrated in a testbed using baseband signal generators, coherent receiver channels, and channel emulators with propagation impairment models derived from experimental testing.

Index Terms — Polarization, Zero Forcing, Suppression, Channel Estimation.

I. INTRODUCTION

As pressures for efficient spectrum utilization mount and wireless system densities increase, wireless systems will be challenged to more effectively operate in environments with interference, including both cooperative interference (e.g., interference signals with known signal properties) and uncooperative interference. Interference suppression techniques are likely to play a prominent role to advance these goals in future systems. While a vast amount of literature exists that deals with interference suppression techniques, most of these techniques cannot efficiently and/or effectively operate against wideband, asynchronous, co-directional interference in severe multipath channels with time-varying interference profiles. For example, conventional adaptive arrays are applicable to the narrowband regime and offer little capability for codirectional interference. In his seminal paper, Winters [1] has shown that for flat fading mobile channels useful suppression levels are possible if a large number of antennas are available and if interference and desired signal components are resolvable in angle. Space-time architectures, which augment conventional arrays to enable wideband processing, also do not have faculties to deal with

codirectional interference except under special circumstances [2].

One architecture that has shown effectiveness to address co-directional interference is the polarization-based suppression architecture. For the narrowband signal case, Compton [3] has shown that when two signals arrive at an array from very closely spaced incidence angles, a space-based array will have difficulty resolving, and hence suppressing, the signals. But if these same signals have distinct polarizations, techniques such as polarization-based Wiener filtering or zero-forcing (ZF) can be used to help resolve the signals [4]. Recent work in polarization channel sounding and polarization modeling [5] suggests that frequency-dependent polarization state differences will generally occur in multipath channels due to polarization mode dispersion.

In [6], Walkenhorst et al. have shown that Compton's techniques can be applied to wider-band co-directional signals in dispersive channels through subband processing. In that work, covariance matrices derived from ideal channel estimates were assumed and used with Wiener filtering to demonstrate the efficacy of the subbanded polarization suppression strategy. We consider a similar approach, but employ ZF filtering instead of MMSE to accommodate asynchronous signals and time varying interference topologies that would pose great challenges to MMSE systems, particularly when the interference profile is different from the profile used to train the adaptive suppression weights.

A ZF-based signal processing architecture to accommodate dynamic interference environments is proposed in [7]. The architecture enables simultaneous use of polarization for diversity via selection combining, single interferer suppression, diversity suppression, and multi-interferer cancellation. The ZF architecture is channel driven so that suppression and diversity processing in asynchronous, time-varying interference environments can be accommodated as long as channel state information for the interference signals are obtained within the last T_c seconds (e.g., with the signals in the clear), where T_c is the channel coherence time. Hence if "valid" channel estimates for the interferers are available, the interference can be suppressed to facilitate potential recovery of desired signals in the environment.

In the case of cooperative OFDM ACCI signals, where a preamble or pilot is known, channel estimation can be achieved using conventional demodulator processing when the signal is in the clear, for example through use of a known preamble. For other forms of interference, such as uncooperative interference, conventional channel estimation is no longer an option, and suboptimal channel estimation

This work was sponsored by the Defense Advanced Research Projects Agency under Contract N66001-10-C-2003. Approved for Public Release. Distribution Unlimited

techniques have to be employed when these signals are in the clear. We propose the use of *relative CSI* estimation that is derived from the Wolf coherency matrix [8] of the received polarimetric signal components.

In either case, during the channel estimation process, if BCCI signals are also in the environment, these can degrade both forms of the channel estimate and the resulting cancellation performance of the ZF filter. We consider the impact of this weak interference on ACCI channel estimates and on the cancellation performance of the associated ZF filter.

Two methods are proposed for counteracting the limitations imposed by the presence of the BCCI during channel estimation. First, a method for detecting the presence of interference is proposed that monitors signal depolarization of the ACCI signal. This measure provides a means to select the channel estimate formed within the last T_c seconds leading to the highest polarization purity and to the best cancellation performance. A second strategy is also considered that mitigates the impact of the interference by exploiting signal polarization correlations in polarization-frequency space. The approach involves a smoothing of the Stokes parameters associated with the channel estimates and is found to yield substantial cancellation ratio gains.

The remainder of this paper is organized as follows. In Section II, signal models are described, including the OFDM signal models, channel models and channel estimation and relative channel estimation techniques. Zero forcing is developed in Section III along with performance measures, and the theoretical impact of imperfect channel estimation effects on ideal ZF cancellation is shown. The section also discusses various factors leading to non-ideal channel estimates, such as estimation of relative CSI for uncooperative interference and factors for ACCI. In Section IV, a polarimetric testbed is described that enables evaluation of the suppression algorithms in emulated channels, where the channel impulse responses were derived from channel sounding experiments. The testbed is applied in Section V to estimate ZF cancellation performance of ACCI in the presence of BCCI. Strategies to mitigate the impact of the BCCI are considered in Sections VI and VII. Polarization-frequency smoothing is addressed in Section VI. In Section VII, an alternative approach based on channel estimation selection from a collection of channel estimates is also proposed, where the best estimate is employed to enhance suppression performance. The paper ends with our conclusions.

II. SIGNAL MODEL

Assume two OFDM-based co-channel signals, where one is a desired signal, and one is the ACCI:

$$s_D(t) = CQ^H x_D \in \mathbb{C}^{N+L} \quad (1)$$

and

$$s_I(t) = CQ^H x_I \in \mathbb{C}^{N+L} \quad (2)$$

where x_I and x_D are the frequency domain OFDM payloads, Q is the DFT matrix and C adds the cyclic prefix. The signals $s_D(t)$ and $s_I(t)$ propagate through polarimetric vector channels

\underline{h}_D and \underline{h}_I , respectively, to yield the signal vectors $\underline{y}_D(t)$ and $\underline{y}_I(t)$ at the output of the channel. At the receiver, after synchronization, removal of the cyclic prefix, and application of the FFT, we may represent the received vector for each signal as a function of the subcarrier index as follows:

$$\underline{Y}_D(k) = \begin{bmatrix} Y_D^v(k) & Y_D^h(k) \end{bmatrix}^T = \underline{H}_D(k) x_D(k) \quad (3)$$

and

$$\underline{Y}_I(k) = \begin{bmatrix} Y_I^v(k) & Y_I^h(k) \end{bmatrix}^T = \underline{H}_I(k) x_I(k) \quad (4)$$

where the superscripts v and h represent orthogonally polarized signal components. We assume that $\underline{Y}_D(k)$ and $\underline{Y}_I(k)$ are not time coincident at the receiver at all times, and hence there is opportunity to estimate their respective channel vectors states when the signals do not overlap. Therefore, channel estimates for each subcarrier associated with H_D and H_I may be obtained. We denote the true vector channel gains associated with subcarrier k by

$$H_D(k) = [H_D^v(k) \ H_D^h(k)]^T \quad (5)$$

and

$$H_I(k) = [H_I^v(k) \ H_I^h(k)]^T. \quad (6)$$

and their estimates by $\hat{H}_D(k)$ and $\hat{H}_I(k)$. These channel estimates remain valid over the coherence time of the channel, designated as T_c , which we assume to be valid for the transmission of several packets.

For interference signals that are not known by the receiver, an alternative channel estimation process is possible that is based on the Wolf coherency matrix. From the coherency matrix

$$C_I(k) = \begin{bmatrix} C_{11}^I(k) & C_{12}^I(k) \\ C_{21}^I(k) & C_{22}^I(k) \end{bmatrix} = \begin{bmatrix} \langle |Y_I^v(k)|^2 \rangle & \langle Y_I^v(k) (Y_I^h(k))^* \rangle \\ \langle Y_I^h(k) (Y_I^v(k))^* \rangle & \langle |Y_I^h(k)|^2 \rangle \end{bmatrix} \quad (7)$$

the relative channel state estimates may be obtained using

$$\tilde{H}_{rel}(k) = C_{12}^I(k) / C_{22}^I(k) \quad (8)$$

The relative CSI yields channel estimates that reflect the relative amplitude and phase between the two orthogonally-polarized components at each subcarrier frequency. These estimates can be used directly in the zero forcing algorithms for interference suppression. The estimates generally require additional sample support to compensate for the impact of errors introduced by the absence of a cyclic prefix. The origins of these errors are presented in the Appendix.

III. ZERO FORCING

With channel estimates for the interference sources in hand, zero-forcing may readily be applied to suppress the interference on a subcarrier-by-subcarrier basis. The output of the ZF suppression filter for subcarrier k is given by

$$Z(k) = W^T(k) Y(k) \quad (9)$$

where

$$W(k) = [H_I^h(k) \ -H_I^v(k)]^T. \quad (10)$$

This filter can be directly applied to the received signal to cancel the interference without need for synchronization and independently of whether or not the desired signal is present. Complete suppression is usually not possible in the polarimetric dimension because the polarization state may exhibit depolarization in each subband, and hence all of the interference energy will not be entirely suppressed. Suppression is also dictated by the quality of the channel estimates. For any subcarrier, if the vector channel estimate associated with the polarization is in error by a central angle ε degrees on the Poincare Sphere [9], then suppression degradation occurs as shown in Figure 1. The maximum cancellation ratio that can be achieved for different polarization separations, ϕ , between the desired and interference signals is represented on the abscissa in the figure, where 0 degrees corresponds to identical states of polarization, and 180 degrees corresponds to orthogonal polarization. The cancellation ratio is defined as:

$$\rho_{dB} = 10 \log_{10} \left(\frac{P_D^{out} / P_I^{out}}{P_D^{in} / P_I^{in}} \right), \quad (11)$$

where P_D^{out} and P_I^{out} correspond to the power of the desired and interference signals at the output of the ZF filter, and where P_D^{in} and P_I^{in} denote the desired and interference signal powers at the input to the ZF filter. The computed cancellation ratios shown in Figure 1 assume identical source powers at the input to the ZF filter and are derived from

$$\rho_\varepsilon = 10 \log_{10} (\sin^2(\varepsilon/2) / \sin^2(\phi/2)), \quad |\phi| > |\varepsilon| \quad (12)$$

The maximum cancellation ratio is seen to exhibit a floor that depends upon the magnitude of the error associated with the quality of the channel estimates.

There are various ways that the quality of the channel estimates can depart from ideal. For uncooperative interference, a channel estimate is formed using relative CSI, which tends to be noisier than CSI estimates derived in conventional channel estimation processing. ZF-based suppression of uncooperative interference is briefly considered here for the case of a 5-tap channel with uncorrelated V and H responses. We assume broad sample support (e.g., 100,000 samples), thus enabling high fidelity estimates of the relative channel estimates. For the given sample support, we compute the complementary CDF of the cancellation performance of a zero forcing filter with N_f subbands. The results are shown in Figure 2. For small N_f , more samples are available per subband to improve the channel estimate, but substantial depolarization is likely to occur over the subband due to the large subcarrier bandwidth. For higher N_f , less depolarization occurs in each subband, but fewer samples per subband are available for estimation. The tradeoff between these two competing factors is evident in the figure.

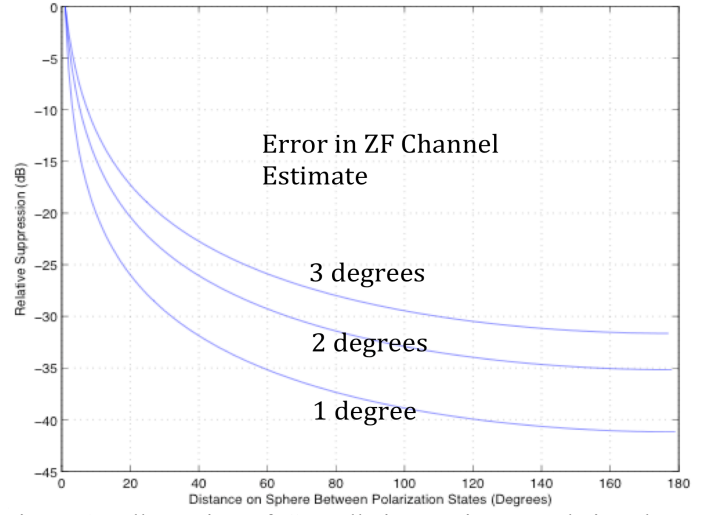


Figure 1. Illustration of Cancellation Ratio Degradation due to Channel Estimation Error for Different Source/Interference Polarization Separation

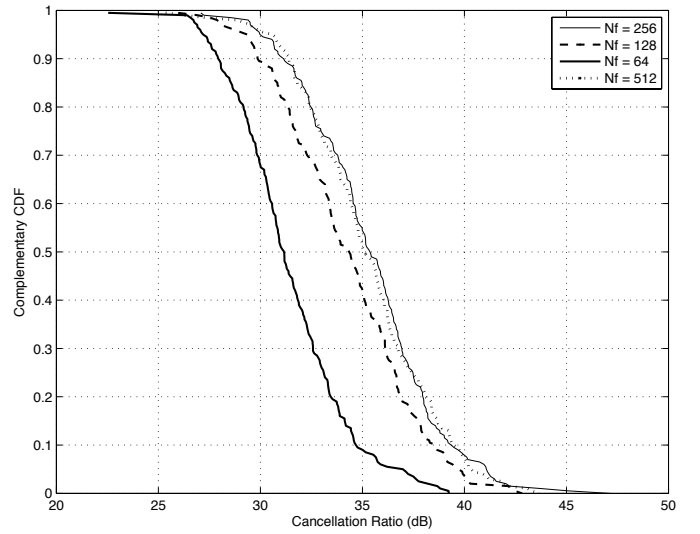


Figure 2. Complementary CDF of Cancellation Ratios using Relative CSI with 10,000 Samples for Training. The sources were assumed to be filtered complex noise.

For ACCI interference, the quality of the channel estimates departs from ideal for a number of reasons. First, estimates are limited by receiver noise, and the quality of the channel estimates degrade as the SNR levels diminish. Second, as with channel estimation for uncooperative interference, errors may result if subcarrier bandwidths used in the ZF scheme are selected to be too large, i.e., when the subcarrier signals exhibit some frequency selectivity. In this case, the polarization will vary within the subcarrier, leading to a floor in the achievable cancellation ratio. Finally, if BCCI is present during channel estimation, the BCCI will impose a floor on achievable cancellation ratios. Depending upon the power level of the BCCI, suppression performance can be substantially degraded. In the remainder of the paper, with the aid of a polarimetric testbed, cancellation limitations imposed by BCCI are explored and avenues to mitigate the impact of BCCI are evaluated.

IV. POLARIMETRIC TESTBED

A polarimetric testbed, shown in Figure 3, was integrated to test and evaluate zero forcing suppression of ACCI signals. The major instrumentation in the testbed include an Agilent Technologies N5106A MIMO Baseband Signal Generator and Channel Emulator (otherwise referred to as the PXB), an Agilent Technologies DSO90000 class multi-channel digital sampling scope that provides wideband coherent reception, and an HP Z800 workstation. The testbed offers capability to: 1) load arbitrary waveforms developed in Matlab into a baseband generator; 2) “transmit” the loaded waveform through an emulated polarimetric 2x2 MIMO channel; 3) generate in-phase and quadrature baseband analog signals at the output of the channel emulator; 4) coherently receive wideband MIMO analog signals using a digital sampling scope; 5) port the received signals into a Matlab/Simulink environment; and 6) apply digital signal processing algorithms in Simulink.

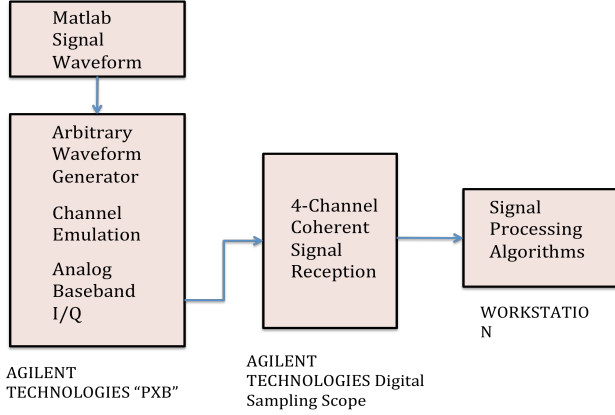


Figure 3. Polarimetric Testbed System Diagram

Using this set-up, ACCI signal packets composed of 12 OFDM symbols were synthesized in Matlab and loaded into the Agilent PXB Baseband Generator. Waveform parameters associated with the ACCI signals are shown in Table 1. The PXB was used to generate these signals at baseband, where polarimetric channel effects were applied via the built-in channel emulator functions of the PXB. Analog in-phase (I) and quadrature (Q) baseband signals corresponding to vertically and horizontally-polarized components were generated at the output of the emulator and passed to a 4-channel receiver, where the signal was digitized. The collected signals were exported to the Matlab/Simulink environment, where the signal processing algorithms were applied.

Table 1. OFDM System Parameters

FFT block size	4096
Cyclic prefix length	1024
OFDM symbol size	5120
Number of data-carrying subcarriers	3200
Carrier frequency	2441.5 MHz
Signal bandwidth	78.125 MHz
Sample rate	100 Msamples/s
Modulation	QPSK

V. CANCELLATION PERFORMANCE

Using the testbed, we investigated the suppression performance of zero forcing in the presence of an interfering OFDM signal during channel estimation, where the relative power between each ACCI signal and the BCCI signal was varied between -40 dB and 0 dB. Figure 4 shows the cancellation ratios that were achieved as a function of the power ratio. The cancellation ratio is seen to degrade linearly with the log of the power ratio. It is noted that the achieved ratios are better than would have been achieved with receiver noise at the same power level. This is due to the fact that the BCCI is polarized and therefore the suppression level will depend upon the specific polarization behavior of the BCCI. In the next two sections, we propose methods to mitigate the effects of BCCI by exploiting polarization-frequency correlations to improve channel estimates and thus, cancellation ratios. One approach is based on channel estimate smoothing in the polarization-frequency dimension. The second approach operates under the premise that multiple channel estimates are available within the last T_c seconds. The approach employs a detector to identify the channel estimate within this collection deemed to provide the best channel estimate based on polarization decorrelation properties.

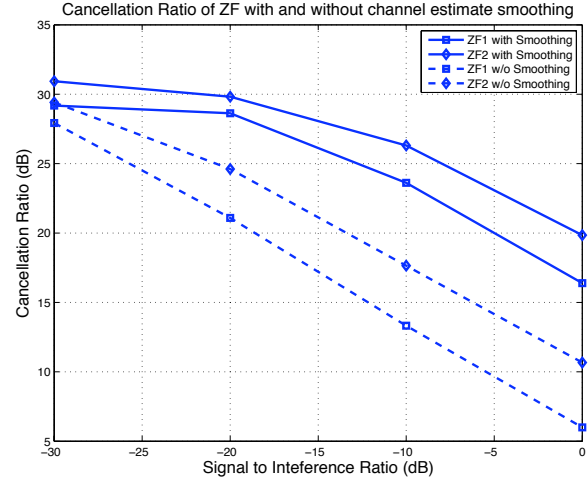


Figure 4. Cancellation Ratios Achieved in the presence of Interference with and without polarization-frequency smoothing.

VI. POLARIZATION-FREQUENCY SMOOTHING

To counter the impact of interference on the channel estimate, we propose to exploit correlations that exist in the polarization-frequency domain. The interference has the effect of inducing perturbations in the nominal polarization state estimate associated with each subcarrier frequency. Figure 5 provides examples of the nominal S2 Stokes parameters in the absence of interference but with a -38 dB noise floor relative to the desired signal power, and corresponding Stokes parameter deviations from nominal for the cases when the interference is present at relative power levels of -30 dB, -20 dB, and -10 dB. The channel estimate can be improved by a simple smoothing operation that filters the noise, yielding a polarization estimate that is closer to the true channel estimate. The result of a smoothing operation on

the S2 Stokes parameter deviations is shown in Figure 5 for the different interference power levels. Achieved cancellation ratios with and without smoothing are shown in Figure 4 and indicate that substantial gains, approximately 13 dB in SIR, can be achieved through this simple operation.

VII. BCCI DETECTION

It is evident that high fidelity channel estimates are important to the performance of the ZF technique, and that the presence of weak interference will limit suppression capability even with smoothing. Since channel estimates are drawn from prior packets, one strategy for dealing with the quality of the channel estimates is to select the ‘best’ channel estimate from among those formed within the last T_c seconds. A proposed method for accomplishing this is to estimate the degree of polarization associated with each packet in this set. The packet exhibiting the highest degree of polarization is deemed to be the best channel estimate, provided that the estimate is not stale.

A measure based on the degree of polarization is derived from the frequency-dependent Stokes parameters associated with the channel estimates. The Stokes parameters may be obtained from the channel estimates through the coherency matrix

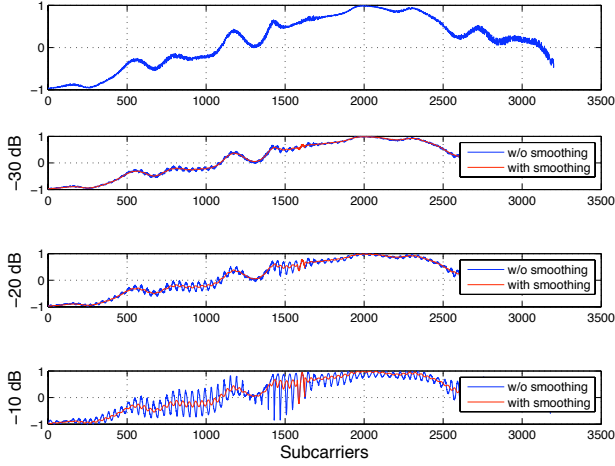


Figure 5. Stokes Parameters for Channel Estimates with and without Interference and with/without Smoothing

$$J(k) = \begin{bmatrix} J_{11}(k) & J_{12}(k) \\ J_{21}(k) & J_{22}(k) \end{bmatrix} = E[\underline{H}_I(k)\underline{H}_I^H(k)] \quad (13)$$

using

$$S(k) = \begin{bmatrix} S_0(k) \\ S_1(k) \\ S_2(k) \\ S_3(k) \end{bmatrix} = \begin{bmatrix} J_{11}(k) + J_{22}(k) \\ J_{11}(k) - J_{22}(k) \\ J_{12}(k)J_{21}^*(k) + J_{21}(k)J_{12}^*(k) \\ j(J_{12}(k)J_{21}^*(k) - J_{21}(k)J_{12}^*(k)) \end{bmatrix} \quad (14)$$

and then normalizing the Stokes parameters by the factor

$$S_{norm}(k) = \sqrt{S_1^2(k) + S_2^2(k) + S_3^2(k)}. \quad (15)$$

A metric based on the normalized S_1 , S_2 , and S_3 parameters that provides an indication of the degree of polarization may be obtained using

$$d_i = \frac{1}{K} \sum_{k=1}^K (\hat{S}_i(k) - \bar{S}_i(k))^2 - \left(\frac{1}{K} \sum_{k=1}^K (\hat{S}_i(k) - \bar{S}_i(k)) \right)^2 \quad (16)$$

where $\bar{S}_i(k)$ is a filtered version of the normalized Stokes parameters, \hat{S}_i , that is used to subtract out the local mean. We note that the resulting measure is a variance of the polarization-frequency residue after the local mean has been subtracted from the original function. The composite metric, d , is formed from the sum of the three Stokes metrics, i.e.,

$$d = \sum_{i=1}^3 d_i. \quad (17)$$

An illustration of metric values for different SIR values is shown in Figure 6. The metric provides correct indication of the packets with the lowest SIR.

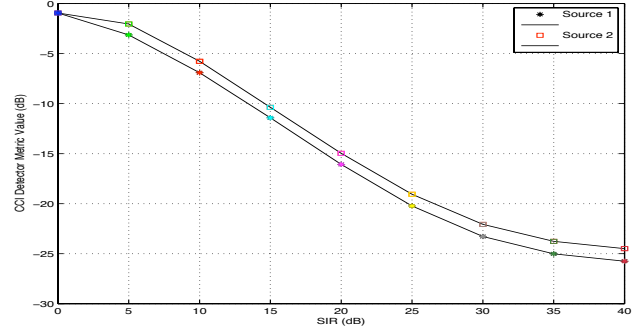


Figure 6. Degree of Polarization Metric versus Relative Interference Power Level

VIII. CONCLUSION

Polarization-based zero forcing filtering is found to enable suppression of wideband co-directional asynchronous signals. The method requires having valid estimates of the channel response associated with the interference, which can be obtained when the interference signal is ‘in the clear’. Channel estimates can be derived using conventional methods if the ACCI signal is demodulated by the receiver or through use of *relative* channel estimates if the ACCI signal is not known. The presence of BCCI during the channel estimation process can severely degrade suppression performance. We demonstrate that in this case, correlations in the polarization-frequency domain can be used to improve cancellation performance. One method involves smoothing of the Stokes parameters, which achieves substantial cancellation performance gains. A second method involves computation of a degree of polarization measure from the polarimetric channel estimates. The measure provides a means to select the ‘best’ channel estimate from among those formed within the last T_c seconds

DISCLAIMER

The views and conclusions contained in this document are those of the authors and should not be interpreted as representing the official policies, either expressed or implied, of the Defense Advanced Research Projects Agency or the U. S. Government.

REFERENCES

1. J. Winters, "Optimum Combining in Digital Mobile Radio with Cochannel Interference," IEEE Journal on Selected Areas in Communications, Vol. 2, No. 4, 1984, pp. 528-539.
2. S.M. Kogon, "Adaptive array processing techniques for terrain scattered interference mitigation," PhD Thesis, Georgia Institute of Technology, 1997.R.
3. Compton, "On the performance of a polarization sensitive adaptive array," IEEE Transactions on Antennas and Propagation, vol. AP-29, No. 5, Sept 1981.
4. D. Stapor, "Optimal receive antenna polarization in the presence of interference and noise," IEEE Transactions on Antennas and Propagation, vol. 43, no. 5, May 1995.
5. T. Pratt, H. Tapse, B. Walkenhorst, and G. Acosta-Marum, "A Modified XPC Characterization for Polarimetric Channels," submitted to IEEE Trans. Vehicular Technology.
6. B. Walkenhorst and T. Pratt, "Polarization-Based Interference Mitigation for OFDM Signals in Channels with Polarization Mode Dispersion," MILCOM08, San Diego, CA. November 17-19, 2008.
7. T. Pratt, H. Tapse, B. Baxley, B. Walkenhorst, and G. Acosta-Marum, "A Polarization-Based Zero Forcing Diversity Suppression Receiver," Submitted to MILCOM 2011.
8. M. Born and E. Wolf, Principles of Optics, Sixth Edition, Pergamon Press, 1980.
9. G. A. Deschamps, "Techniques for Handling Elliptically Polarized Waves with Special Reference to Antennas, Part II - Geometrical Representation of the Polarization of a Plane Electromagnetic Wave," Proc. IRE, Vol. 39, pp. 540-4, May 1951.
10. T. Thomas and F. Vook, "Asynchronous Interference Suppression in Broadband Cyclic-Prefix Communications," IEEE 2003, p. 568-572.

APPENDIX

Let $x(n)$ represent the signal of interest propagating through a polarimetric channel consisting of m multipaths, where \vec{h}_m represents the vector channel response associated with path m . The vector at the output of the channel is given by

$$\vec{y}(n) = \sum_{m=0}^{M-1} \vec{h}_m x(n-m) \quad (18)$$

This may be rewritten as [10]

$$\vec{y}(n) = \sum_{m=0}^{M-1} \vec{h}_m x((n-m)_N) + \sum_{m=0}^{M-1} \vec{h}_m \{x(n-m) - x((n-m)_N)\} 1_{(n-m) < 0} \quad (19)$$

which enables analysis of errors introduced by multipath delay when $x(n)$ does not have a cyclic prefix. Taking the DFT

$$\bar{Y}(k) = \sum_{n=0}^{N-1} \bar{y}(n) e^{-j2\pi kn/N} \quad (20)$$

and using (19), one obtains [10]

$$\begin{aligned} \bar{Y}(k) &= \sum_{n=0}^{N-1} \sum_{m=0}^{M-1} \vec{h}_m x((n-m)_N) e^{-j2\pi kn/N} + \sum_{n=0}^{N-1} \sum_{m=0}^{M-1} \vec{h}_m \{x(n-m) - x((n-m)_N)\} 1_{(n-m) < 0} e^{-j2\pi kn/N} \\ &= \bar{H}(k) X(k) + \sum_{n=0}^{N-1} \sum_{m=0}^{M-1} \vec{h}_m \{x(n-m) - x((n-m)_N)\} 1_{(n-m) < 0} e^{-j2\pi kn/N} \end{aligned} \quad (21)$$

The vertically-polarized component is given by:

$$Y^v(k) = H^v(k) X(k) + \sum_{n=0}^{N-1} \sum_{m=0}^{M-1} h_m^v \{x(n-m) - x((n-m)_N)\} 1_{(n-m) < 0} e^{-j2\pi kn/N}$$

and the horizontally-polarized component by:

$$Y^h(k) = H^h(k) X(k) + \sum_{n=0}^{N-1} \sum_{m=0}^{M-1} h_m^h \{x(n-m) - x((n-m)_N)\} 1_{(n-m) < 0} e^{-j2\pi kn/N}$$

At the receiver, channel estimates are formed using

$$H^v(k) = \frac{Y^v(k)}{X(k)} = H^v(k) + \left(\sum_{n=0}^{N-1} \sum_{m=0}^{M-1} h_m^v \{x(n-m) - x((n-m)_N)\} 1_{(n-m) < 0} e^{-j2\pi kn/N} \right) / X(k)$$

$$H^h(k) = \frac{Y^h(k)}{X(k)} = H^h(k) + \left(\sum_{n=0}^{N-1} \sum_{m=0}^{M-1} h_m^h \{x(n-m) - x((n-m)_N)\} 1_{(n-m) < 0} e^{-j2\pi kn/N} \right) / X(k)$$

which indicates that errors are introduced in multipath channels when $x(n)$ does not have a cyclic prefix. In general, errors are introduced for all paths with delays exceeding the cyclic prefix length. The error terms can be reduced by exploiting correlations in the polarization-frequency domain and may be accomplished through a smoothing of the Stokes parameters associated with the channel estimates (see Section VII for a discussion of smoothing). Applying these channel estimates in ZF suppression and ideal channel estimation, the interference residue after suppression is given by

$$E = \text{IFFT}(H^v)^* y^v(n) - \text{IFFT}(H^v)^* y^h(n) = h_p^h * y^v(n) - h_p^v * y^v(n)$$

where

$$\begin{aligned} h^h * y^v(n) &= \sum_{p=0}^{M-1} h_p^h \sum_{m=0}^{M-1} h_{m-p}^v x((n-m-p)_N) \\ &+ \sum_{p=0}^{M-1} h_p^h \sum_{m=0}^{M-1} h_{m-p}^v \{x(n-m-p) - x((n-m-p)_N)\} 1_{(n-m-p) < 0} \end{aligned}$$

and

$$\begin{aligned} h^v * y^h(n) &= \sum_{p=0}^{M-1} h_p^v \sum_{m=0}^{M-1} h_{m-p}^h x((n-m-p)_N) \\ &+ \sum_{p=0}^{M-1} h_p^v \sum_{m=0}^{M-1} h_{m-p}^h \{x(n-m-p) - x((n-m-p)_N)\} 1_{(n-m-p) < 0} \end{aligned}$$

Hence the residue may be rewritten as:

$$\begin{aligned} E &= h^v * \left(\sum_{m=0}^{M-1} h_m^h x((n-m)_N) + \sum_{m=0}^{M-1} h_m^h \{x(n-m) - x((n-m)_N)\} 1_{(n-m) < 0} \right) \\ &+ h^h * \left(\sum_{m=0}^{M-1} h_m^v x((n-m)_N) + \sum_{m=0}^{M-1} h_m^v \{x(n-m) - x((n-m)_N)\} 1_{(n-m) < 0} \right) \end{aligned}$$

If $\hat{h}^v = h^v$ and $\hat{h}^h = h^h$, then the residue will be approximately zero. Perfect nulling is not anticipated due to depolarization that occurs within each subband.